

# Structural Optimization of a Total Replacement Hip Prosthesis

M. Grasso, F. Penta, G.P. Pucillo, V. Rosiello, A. Piscopo

**Abstract**—Planted articular joints replace bone articulation allowing the transfer of loads and articular displacements. However, hip prosthesis cannot guarantee the same dynamic friction coefficients of natural joints. The present study analyses the main design solutions for hip prosthesis, in terms of geometries and materials and an in-depth bibliographic research was performed to identify the load spectra corresponding to the different operation conditions of the planted joint. The final aim of this study is to analyze the stress state induced in the prosthesis by the mounting effect as well as under the action of loads deriving from ambulation in order to perform a structural optimization which guarantees the needed life time. In order to optimize the chosen prosthesis, the geometry of the three elements constituting the prosthesis was reconstructed through the reverse engineering technique: femoral head, acetabular cup and insert. The geometries obtained were used to implement a finite element 3D model in ANSYS® environment. The results obtained with the finite element 3D model were used as a reference to study the effects of some geometrical parameters of the prosthesis with a simplified model which takes advantage of the geometric axisymmetrical properties of the prosthesis.

**Index Terms**— Hip prosthesis, hyperelastic, total hip replacements, UHMWPE, wear, polyethylene.

## I. INTRODUCTION

Implant interventions of hip joint endoprosthesis are the most common. Endoprostheses are permanent systems which have to be inserted inside the body, into direct contact with the recipient organism tissues in order to completely or partly replace a joint which has lost its functionality. The hip is made up of two solid bodies, bone endings; each of them is covered by an elastic and porous layer, called cartilage. The joint lubrication is guaranteed by the synovia, a viscous liquid composed by plasma containing water with proteins, salt and hyaluronic acid. In normal operating conditions, hydrodynamic lubrication mechanisms limit wear by guaranteeing friction coefficients between 0.005 and 0.025. In case of hip pathologies there is a reduction in the

lubricating capabilities of the synovial fluid with a consequent damage and wear of the joint surfaces and a progressive loss of the joint functionality. The total hip arthroplasty (THA) is an orthopaedic procedure which allows the rehabilitation of the damaged joint by implanting devices which reproduce hip kinematic with an artificial spherical joint [1 - 2].

The current concept of low friction coefficient THA was developed during the sixties by Charnley [3], from whom the name of this type of prosthetic implant derives. This kind of prosthesis includes a prosthetic femoral head having a diameter of about 22mm, settled on a femoral support which is in contact with the acetabular part. From the first Charnley prosthesis different versions have been developed [4]. In the past, prosthesis were entirely made in metal, inserting between the femoral head and the acetabular elements with a low friction coefficient, like alumina. The latter, due to the very low resistance to impacts, has almost been replaced by ultra high molecular weight polyethylene (UHMWPE). It has been commonly accepted [5] that wear is the main cause for ultra high molecular weight polyethylene yielding. Moreover, residues from polyethylene can lead to bones osteolysis and therefore to implant yielding [6]. For this reason it is necessary to know contact pressures which depend, beyond materials, on elements dimensions. In [5] the effects of the interference bone prosthesis were analyzed with an asymmetric flat model without considering the three-dimensionality problem due to the asymmetry of the bone. In [6] the contributions of the bone-prosthesis anchor screws to polyethylene liner wear were experimentally measured, however the test was performed imposing a force which varies in intensity but in a fixed direction, which is not true in all loading conditions. Experimentation improvements were considered in [7] where the contact pressures were measured by varying the loading direction and inserting the prosthesis into a real hip. Squire et al. [8] measured in vivo the forces acting on the insert during common daily activities and the consequence of the initial interference on the wear and damage mechanisms of ceramic inserts. Through a FE model, Gebert et al. [9] analyzed the effects of interference and friction on the primary stability of the prosthesis. Schmidig et al. [10] evaluated the variations of the twisting moment due to the friction force depending on the thickness of the liner insert and the head diameter. Ong et al. [11] evaluated the internal stresses and wear of a prosthetic implant through a finite element three dimensional model in which a particular constitutive model for the polyethylene liner was implemented. Markel et al. [12] determined polyethylene

M. Grasso is with the *Department of Industrial Engineering, University of Naples Federico II*, 80125 ITALY (corresponding author, phone: +390817682452; e-mail: marzio.grasso@unina.it).

F. Penta is with the *Department of Industrial Engineering, University of Naples Federico II*, 80125 ITALY (e-mail: penta@unina.it).

G.P. Pucillo is with the *Department of Industrial Engineering, University of Naples Federico II*, 80125 ITALY (e-mail: gpucillo@unina.it).

V. Rosiello is with the *Department of Industrial Engineering, University of Naples Federico II*, 80125 ITALY (e-mail: vincenzo.rosiello@unina.it).

A. Piscopo is with the *Fatebenefratelli Hospital*, 80120 - Benevento (e-mail: piscopo.antonio@fbfn.it).

liner deformation values through experimental tests on a cadaveric model. Goebel et al. [13] obtained deformation values after the application of the load and the ones due to the initial interference through a FE model for different values of liner thickness. Hua et al. [14] connected the effects of the acetabular cup inclination and wear on the contact surface between a metallic head and a polyethylene insert. Regis et al. [15] studied the possible correlations between oxidation and stress noting that stresses distribution is asymmetric like the one in oxidized surfaces. Using a finite element model, Hua et al. [16] determined the interface stresses between a metallic head and the polyethylene liner at the variation of the inclination angle of the acetabular cup when there is a micro separation between the head and liner.

## II. MATERIALS AND METHOD

The modelled prosthesis is made up of a liner having an internal diameter of 36mm in UHMWPE material, an acetabular cup having an internal diameter of 44mm in titanium alloy, and a prosthesis head mounted on the stalk in chromium-cobalt alloy having the same diameter as the liner, as shown in Fig. 1.

The ultra crosslinked polyethylene (UHMWPE) in question is obtained from the GUR 1050 resin and processed with three irradiation and annealing cycles. During each cycle the resin is irradiated with 30kGy and annealed for 8 hours at 130°C. The aforementioned process allows to remove free radicals, which are present in case of irradiation at 90 kGy in just one cycle.

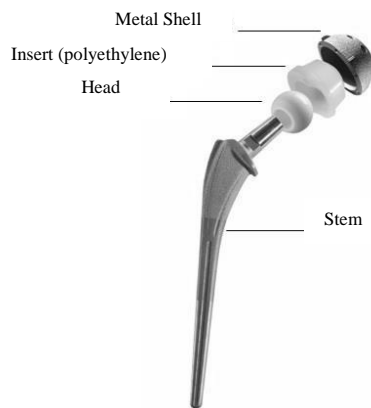


Fig. 1. Example of a hip prosthesis.

Regarding the polyethylene, in Table I values of yield strength, tensile strength and the strain at break before processing are reported. Moreover, in the same table values after a five year ageing are shown.

TABLE I  
YIELD AND TENSILE STRENGTH AND STRAIN AT BREAK VALUES.

	Aged (ASTM 2003)	Yield strength [MPa]	Tensile strength [MPa]	Percentage elongation
UHMWPE	Yes	22.1±0.5	57.0±3.7	418±19
vergin	No	22.7±0.6	57.5±5.5	422±17
UHMWPE worked with three cycles	Yes	23.5±0.3	56.7±2.1	267±7
	No	23.6±0.2	56.3±2.3	266±9

TABLE II  
MECHANICAL CHARACTERIZATION OF METAL SHELL AND HEAD MATERIALS.

	Modulus of elasticity [GPa]	Poisson's modulus	Friction coefficient with the UHMWPE
Titanium alloy	118	0.3	0.086
Chromium-cobalt alloy	210	0.3	0.16

The energy approach is used to characterize polymeric materials with hyperelastic behaviour in the Finite Element Method. It was assumed that the materials are with isotropic and conservative behaviour. All theories developed up to now allow us to identify the elastic energy in function of three stretch ratios along three principal directions. Moreover, energy losses in the form of heat due to hysteresis cycles are neglected. Using these concepts as a starting point, it is possible to find in literature two models: one for materials with an almost incompressible behaviour and one for incompressible materials. Different authors developed this theory to make it accessible in FE codes starting from data collected through material characterizations. It was shown that for a complete determination of the material constants experimental data derived from stress and unconfined compressive strength, pure shear, biaxial and equibiaxial tests are needed.

The most used models are those by Fung, Mooney-Rivlin, Ogden, Polynomial, Yeoh, Arruda-Boyce and Neo-Hookean.

Ogden's model for the case of uniaxial tension or compression has the following form:

$$\sigma_1 = \sum_1^n \mu_p (\lambda_p^\alpha - \lambda^{-\frac{\alpha_p}{2}}) \quad (1)$$

where  $\sigma_1$  is the uniaxial compression,  $\lambda$  is the stretch ratio,  $\mu_p$  and  $\alpha_p$  are constants of the model. By means of curve fitting algorithms it is possible to identify the different constants. The greater the number of constants in the sum, the greater the degree of complexity to which the curve can get. For the purposes of the stability of the stiffness matrix the following conditions need to be satisfied:

$$\mu_p \alpha_p > 0 \text{ for } p = 1, \dots, N \quad (2)$$

$$\sum_1^n \mu_p \alpha_p = 2 \mu \quad (3)$$

Most of the curve fitting codes usually implement also these conditions in their algorithms. The result of the curve fitting corresponding to the Ogden's three-terms coefficients are reported in Table III.

TABLE III  
OGDEN'S CONSTANTS.

	$\mu$	$\alpha$	d
First term	5.8926	1.5663	0.001
Second term	5.5413	1.5591	0.001
Third term	5.4853	1.5696	0.001

The three components of the different loading conditions in the reference femoral system were estimated considering an average patient weighting 80 kg [17 - 18]. Among the several loading conditions identified under the hypothesis above discussed, the simple walk condition was chosen.

The geometry of the hip prosthesis chosen for the present study was scanned with a 3D scanner (3Dshape D700) having a precision of 10 micrometers.

Fig. 2 shows the sequence through which the CAD model was created. The curves obtained by sectioning the external surfaces, which were obtained using the scanner, with two symmetry planes were exported. These curves were smoothed allowing to convert the splines in circumferences and straight lines. In this way, when solids were created the external surfaces, having spherical shapes and therefore perfectly matched with each other, were created.

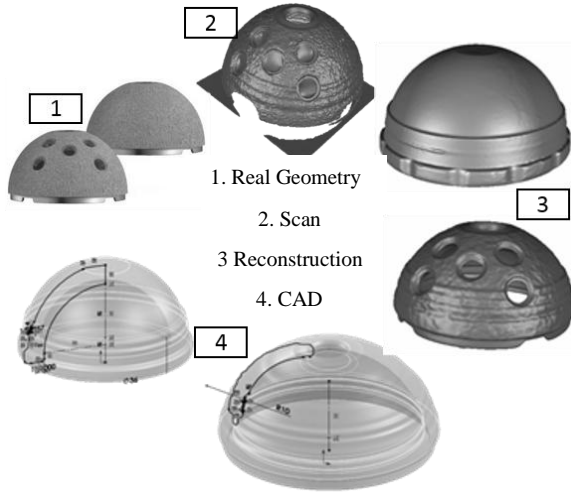


Fig. 2. From Real Geometry to the CAD.

Once the matching was defined, than it was possible to observe that:

- on the area highlighted in Fig. 4(b), interference takes place;
- the liner presents a protuberance which connects to the metal shell;
- all remaining surfaces are constructed in order to match perfectly each others.

### III. FEM ANALYSIS

The geometry was used to implement a FEM analysis in Ansys®.

The femoral head model, the liner and metal shell were discretized using solid elements. It was not possible to use the axisymmetric properties of the prosthesis as forces are not symmetrical. It was decided to use solid element with 8 nodes to discretize the prosthesis. With this element it is possible to consider non linear effects such as large displacements and implement the mixed U-P formulation. Both these options are needed in combination with hyperelastic materials to avoid volumetric locking problems. As a matter of fact, for all materials having a Poisson's ratio of about 0.5, that is to say materials are incompressible or near uncompressible, when they are used with linear solid elements a stiffness which is higher than the real one appears. The stress state can be subdivided into deviatoric and volumetric component. The latter component depends on the bulk modulus which for Poisson's ratios equal to 0.5 tends to infinity overrating the element stiffness as given in Equation (4).

$$\kappa = \frac{E}{3(1-2\nu)} \quad (4)$$

Referring to the fully integrated solid element with 8 nodes, for each node the degrees of freedom referred to the volumetric variation were constrained, since the volume is

constant for incompressible materials. In order to avoid this problem, for the liner element only, the mixed U-P formulation was used. In this case the degrees of freedom referred to volumetric variation are treated separately through the introduction of Lagrange multipliers. The consequences are the following: increase in size of the stiffness matrix [K] and consequent increase in the computational time.

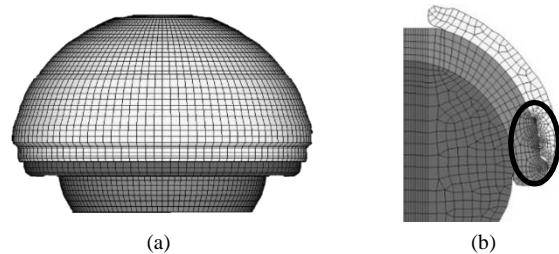


Fig. 3. (a) Entire model and (b) section of the mesh.

In order to obtain a more accurate solution and in particular to the reduce penetrations, it was decided to match the nodes of the surfaces in contact. The size of the elements in the interference area is 0.2mm instead of 1.5mm adopted for the remaining part.

The entire model is reported in Fig. 3(a). The model is made of 130486 elements and 145280 nodes. The mesh of the final model was obtained interactively by simulating models with smaller angular dimensions to check which discretization gives the best results in terms of final penetration and press-fit resolution.

In order to allow the application of the load, at the centre of the head a rigid region was created Fig. 4(a). These constraint equations allow creating a relation among all degrees of freedom.

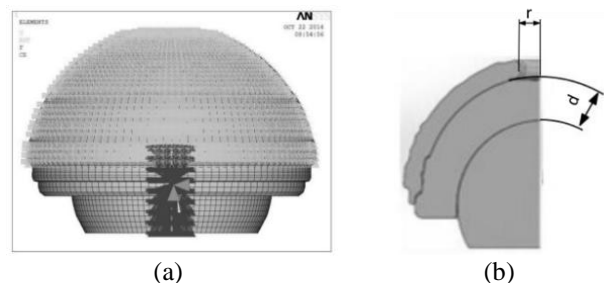


Fig. 4. (a) Full model with rigid region, (b) liner parameters.

The head-liner and liner-metal shell contacts were simulated using the penalty approach. Both liner surfaces were chosen as contacts, since polyethylene is much more deformable than metal. Between liner and head it was defined a friction coefficient equal to 0.16, while between liner and metal shell it is set to 0.086 [11].

At the end, the optimization parameters were chosen. With respect to the geometry of the initial prosthesis, the thicknesses and opening range of the metal shell were varied. The thickness was increased by varying only the head diameter (Fig. 4(b)).

This because the external diameter of the metal shell, is a clinic parameter, therefore it was decided to observe what happens when smaller head diameters are used. In addition to the initial diameter equal to 36 mm, other values equal to 22, 26, 28 and 32 mm were considered.

Conversely, concerning the contact area of the metal shell the openings were modified as reported in Fig. 4(b) varying

the initial radius of 6.3mm. The tested radii are: 3, 5 and 8 mm.

#### IV. RESULTS

Determining the mounting effect is important because in the lifting conditions, when the weight of the body does not affect the hip, the only stresses acting are the ones derived from the interference. Fig. 6 shows the contour plot of the total displacements for the solid model. From the plot it can be seen that the liner is more deformable and that it absorbs the majority of deformations. From the map of total displacements (Fig. 5) it can be seen that the maximum displacement is in the interference area. The metal shell and the head, being more rigid than the liner, have much smaller total displacements. The value of maximum displacement is 0.23mm.

The regions affected by the greater value of the total displacement are located close to the contact area. In this zone the liner is free to deform as it has no constraints. In particular, observing the contour plot of the total displacement focusing the attention on the liner component, it can be seen that the material is pushed towards the outside. This is due to the compression that the metal shell applies through the interference areas. In the metal shell, displacements are concentrated in the bottom area. At this zone the cross section is smaller and not constrained being more prone to deformable.

Hydrostatic stress is reached in correspondence of the interference areas. In the bottom part of the bead element tensile stresses arise. This is due to the fact that the material under the bead can freely flow downwards as it is not constrained, whilst the upper part does. The von Mises equivalent stress values in the metal shell, which is the component with the highest elastic modulus, in correspondence of the interference area.

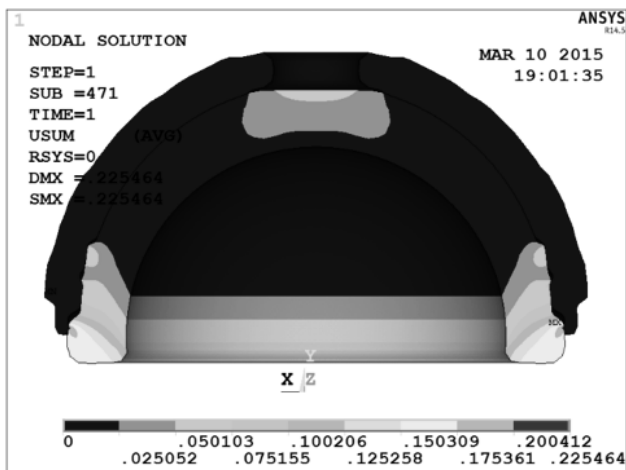


Fig. 5. Contour plot of the total displacements.

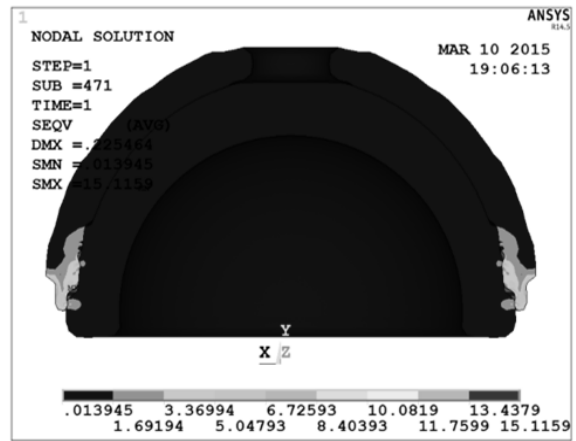


Fig. 6. Contour plot of the equivalent von Mises stress.

Under the action of the maximum load, most of the deformations are concentrated in the liner, which is the most deformable component of the prosthesis (Fig. 7). It can be clearly noted that the stress, displacement and strain contours are not symmetric. This is due to the fact that the force has components in all three directions. In the upper part, liner-hole of the metal shell contact, and in the bottom part, intersection area, displacements reach the maximum value equal to 0.341 mm. This high value is due to the fact that, in the interference area, it is applied a load which tends to compress even more the liner on the face of the metal shell.

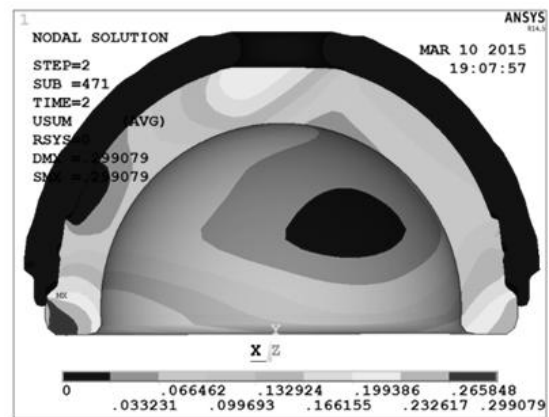


Fig. 7. Contour plot of total displacement under service load.

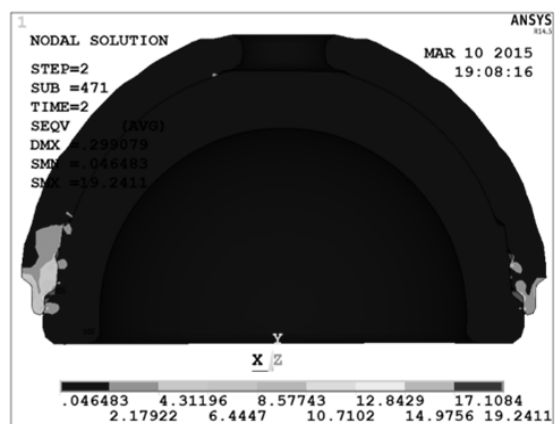


Fig. 8. Contour plot of the equivalent von Mises stress under service load.

In the upper part, the liner is crushed on the edge of the metal shell hole. Along the loading line the liner is pressed

on the internal face of the metal shell, creating a hydrostatic state.

The maximum values of the von Mises equivalent stress (Fig. 8) are achieved at the fitting area due to the overlapping of the mounting effects and the external load.

The contour plot of the equivalent stresses in the liner component shows the presence of three peaks, which are all located on the plane containing both the symmetry axis and the force. The three peaks are located in correspondence of the two singularities, which are at the upper edge of the truncated cone area and at the lower part of the bead, as well as in the area of maximum interference.

The contact pressure between liner and head is very important as it determines the liner wear rate. On the basis of data available in literature, it can be observed that the area most affected by the wear corresponds to the area interested by the maximum contact stress peak [19]. Even though the contact pressure between the liner and the metal shell is higher, this does not imply wear because between the two elements there is not relative motion.

Contour plot of the von Mises equivalent strain shows that, even though there cannot be abrasive wear phenomena, the strain gradient could create wear problems because of fretting between liner and metal shell.

The analysis of the effects produced by the geometry variations underlined which parameters affect the stress state. In particular, a decrease in the liner diameter values as the contact surface between head and liner increases has been observed. Under the action of the same load the decrease of the liner diameter values implies that:

- higher stresses at the liner/head interface occur;
- higher stresses at the liner/metal shell interface in the upper part occur;
- maximum stress decreases.

Fig. 10 shows the variations of the stress state in function of liner thickness. In particular, it can be seen that decreasing the head diameter then the contact pressure on the internal surface of the liner increases. This effect produces an increase in abrasive wear which depends on the normal contact pressure. Moreover, smaller values of the radius reduce the range of motion. Such disadvantages make it believe that unless there are anatomic problems, the prosthesis to be used is the one having the minimum thickness of the liner. In correspondence of the bead, it can be noted that the maximum equivalent stress values increase as the liner thickness increase (Fig. 11).

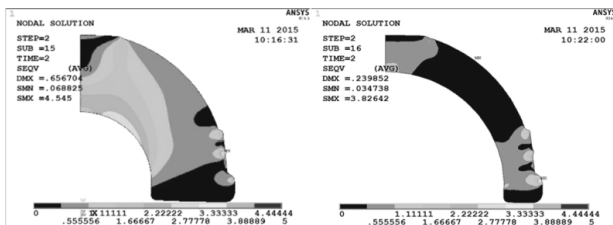


Fig. 9. Differences in the contour plot of the equivalent von Mises stress for two different thickness values.

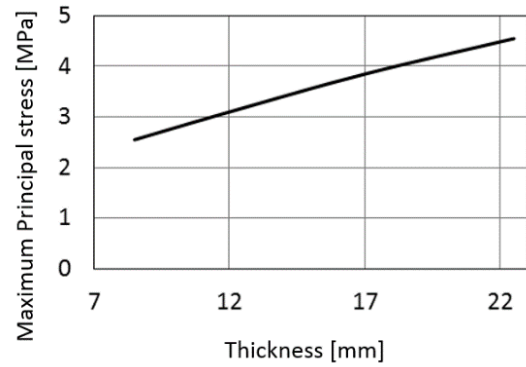


Fig. 10. Variation of the stress state in function of thickness.

Regarding the effects produced by the variation of the opening radius values, it can be seen that:

- the stress peak in the upper part of the contact between liner and metal shell increases as the opening radius values increase, moreover the peak moves following the opening;
- the stress state in correspondence of the interference area does not vary;
- the maximum stress at the interface between head and liner increases.

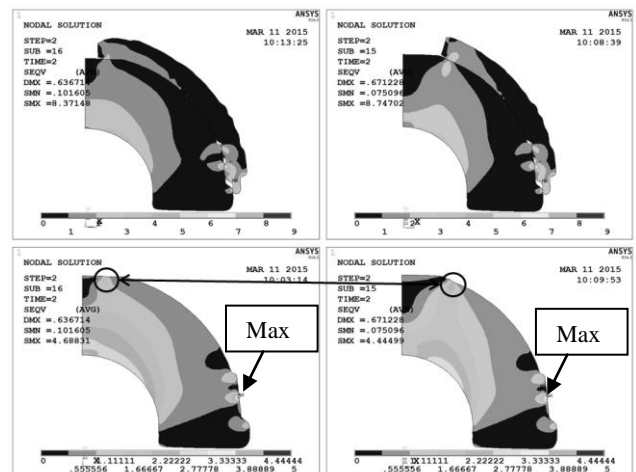


Fig. 11. Differences in the contour plot of the equivalent von Mises stress for two different radius values.

At the end of the optimization process, it is clear that the liner having smaller thickness and the minimum opening radius of the metal shell represents the best compromise. The upper opening of the metal shell affects the contact surface between the insert and the acetabular cup. This hole is used to centre the metal shell before positioning the insert and, in case they are needed, the fixing screws. Commercially there are different centring systems which allow to completely dismissing the idea to use a central hole; this would make stress distribution more uniform, as it was seen in the analyses.

The maximum equivalent von Mises stress for different values of the thickness and opening radius used in this work is reported in Fig. 12.

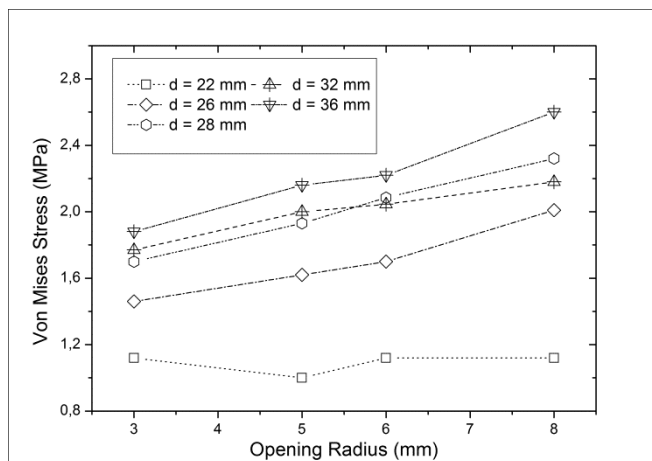


Fig. 12. Equivalent von Mises stress in function of the metal shell opening radius.

The values of the opening radius evaluated in the present research are equal to 3, 5, 6 (the initial one) and 8 mm. It should be noted that, for values of the opening radius up to 5 mm, the contact area is located in correspondence of the flat part of the liner external surface. On the other end, for values greater than 5 mm contact takes place in the spherical part of the external liner surface.

#### V. CONCLUSION

In the present paper, the materials commonly used in endoprosthesis were analyzed, underlining advantages and disadvantages related to their use. Among the most common material adopted in the production of prosthesis inserts, UHMWPE polyethylene is today widely used. On the basis of a preliminary bibliographical survey, the loading conditions under which the prosthesis of a person having an average weight equal to 80 kg were described. The geometry was rebuilt through a reverse engineering method. The effects of fitting and service loads on the structural response of the prosthesis and in particular of its weaker component, the liner, were studied. The achieved results highlighted the crucial role on the structural assessment of the prosthesis played by the fitting stresses, which are of the same order of magnitude than those due to the service load. In the areas close to both the bead and the metal shell hole, there were remarkable stress concentrations. Moreover, using a simplified model, the effect produced by the thickness values on the stress state was evaluated. It was noted that, as the thickness values increase the stress peak value increases, moving from the lower to the upper part of the contact area between the liner and the metal shell. Moreover, as the opening radius values increase the maximum stress values increase, due to the reduction of the total contact surface. Modifying the geometry of the bead a better stress path and a decrease in the maximum stress peak values was achieved. This last change really made improvements, even though its feasibility should be checked. We were unable to study the fatigue behaviour of the product due to the lack of lab experimental data on these particular components on the material itself used for the liner.

#### ACKNOWLEDGMENT

The authors greatly acknowledge the support provided by Eng. Luigi Macera for the reconstruction of hip prosthesis by means of the reverse engineering technique.

#### REFERENCES

- [1] R. Pietrabissa. "Biomateriali per protesi e organi artificiali: introduzione alla biocompatibilità, alla scienza e all'applicazione dei materiali per dispositivi biomedici". Patron, 1996.
- [2] J. R. Foran and S. J. Fischer. "Total Hip Replacement". December 2011.
- [3] Charnley J. "Arthroplasty of the hip: a new operation". The Lancet. 1961;277(7187):1129-1132.
- [4] J. S. Siopack e H. E. Jergesen. "Total Hip Arthroplasty". West J Med, San Francisco, California, 1995.
- [5] X. Hua, B. M. Wroblewski, Z. jin and L. Wang. "The effect of cup inclination and wear on the contact mechanics and cement fixation for ultra high molecular weight polyethylene total hip replacements". Medical Engineering and Physics, 34, pp. 318-3, 2012.
- [6] C. Khalily, M. Tanner, V. Williams and L. A. Whiteside. "Effect of locking mechanism on fluid and particle flow through modular acetabular components". Journal of Arthroplasty, vol. 13, n. 3, 1988.
- [7] K. H. Widmer, B. Zurfluh and E. W. Morscher. "Load Transfer and Fixation Mode of Press-Fit Acetabular Sockets". Journal of Arthroplasty, vol. 17, n. 7, 2002.
- [8] M. squire, W. Griffin, B. Mason, R. Peindl and S. Odum. "Acetabular Component Deformation with Press-Fit Fixation". The journal of Arthroplasty, vol. 21, n. 6, 2006.
- [9] A. Gebert, J. Peters, N. Bishop, F. Westphal and M. Morlock. "Influence of press-fit parameters on the primary stability of uncemented femoral resurfacing implants". Medical Engineering & Physics, vol. 31, pp. 160-164, 2009.
- [10] G. Schmidig, A. Patel, I. Liepins, M. Thakore and D. C. Markel. "The effect of acetabular shell deformation and liner thickness on frictional torque in ultrahigh-molecular-weight polyethylene acetabular bearings". The Journal of Arthroplasty, vol. 25, n. 4, pp. 644-653, 2010.
- [11] K. L. Ong, S. Rundell, I. Liepins, R. Laurent, D. Markel and S. M. Kurtz. "Biomechanical Modeling of Acetabular Component Polyethylene Stresses, Fracture Risk, and Wear Rate following Press-Fit Implantation". Journal of Orthopaedic Research, vol. 27, pp. 1467-1472, 2009.
- [12] D. Markel, J. Day, R. Siskey, I. Liepins, S. Kurtz and K. Ong. "Deformation of metal-backed acetabular components and the impact of liner thickness in a cadaveric model". International Orthopedics, pp. 1131-1137, 2011.
- [13] P. Goebel, D. Kluess, J. Widing, R. Souffrant, H. Heyer, M. Sander and R. Bader. "The influence of head diameter and wall thickness on deformation of metallic acetabular press-fit cups and UHMWPE liners: a finite element analysis". Journal of Orthopedic science, vol. 18, pp. 264-270, 2013.
- [14] X. Hua, B. Wroblewski, Z. Jin and L. Wang. "The effect of cup inclination and wear on the contact mechanics and cement fixation of ultrahigh molecular weight polyethylene total hip replacements". Medical engineering & Physics, vol. 34, pp. 318-325, 2012.
- [15] M. Regis, P. Bracco, L. Giorgini, S. Fusi, P. Dalla Pria, L. Costa and C. Schmid. "Correlation between in vivo stresses and oxidation of UHMWPE in total hip arthroplasty". Journal of material science, n. 25, pp. 2185-2192, 2014.
- [16] X. Hua, J. LI, L. Wang, Z. Jin, R. Wilcox and J. Fisher. "Contact mechanics of modular metal-on-polyethylene total hip replacement under adverse edge loading conditions". Journal of Biomechanics, n. 47, pp. 3303-3309, 2014.
- [17] M. Heller, G. Bergmann, J.-P. Kassi, L. Claes, N. Haas and G. Duda. Determination of muscle loading at the hip joint for use in pre-clinical testing. Journal of Biomechanics, vol. 5, n. 38, pp. 1155-1163, 2005.
- [18] G. Bergmann, G. Deuretzbacher, M. Heller, F. Graichen, A. Rohlmann, J. Strauss and G. Strauss. "Hip contact forces and gait patterns from routine activities". Journal of Biomechanics, vol. 7, n. 34, pp. 859-871, 2001.
- [19] S. M. Kurtz. "UHMWPE Biomaterials Handbook (Second Edition)". Boston: Academic Press, 2009.

Latest modifications sent by email on the 23 July 2015.

According to the last reviewer's requests images have been resized in order to fit the pages' borders.

**Last modification sent by email on the 03 June 2015**

**According to the reviewer's requests the text has been modified and, where needed, references have been added. All changes have been done in accordance with the scanned document sent to the Authors on the 3 June 2015. The framework of the paper remained the same.**